J Electr Eng Technol.2015; 10(3): 1275-1283
http://dx.doi.org/10.5370/JEET.2015.10.3.1275

ISSN(Print) 1975-0102
ISSN(Online) 2093-7423

Markov Chain of Active Tracking in a Radar System and Its Application to Quantitative Analysis on Track Formation Range

Chang-Soo Ahn*, Ji-Eun Roh, Seon-Joo Kim**, Young-Sik Kim*** and Juseop Lee†**

Abstract – Markov chains for active tracking which assigns additional track illuminations evenly between search illuminations for a radar system are presented in this article. And some quantitative analyses on track formation range are discussed by using them. Compared with track-while-search (TWS) tracking that uses scan-to-scan correlation at search illuminations for tracking of a target, active tracking has shown the maximum improvement in track formation range of about 27.6%. It is also shown that the number and detection probability of additional track beams have impact on the track formation range. For the consideration of radar resource management at the preliminary radar system design stage, the presented analysis method can be used easily without the need of Monte Carlo simulation.

Keywords: Markov chain, Radar, Track formation range, Track-while-search, Active tracking

1. Introduction

Compared with the mechanically scanned array (MSA) radar that uses hydraulically or electrically controlled gimbals to physically move the array for search, the electronically scanned array (ESA) radar implements rapid beam steering by independently setting the phase of phase shifters connected to each array element [1].

An ESA radar has improved search and track performance because of the beam agility [2]. However, consideration for resource management in an ESA radar is necessary to have the optimized system performance.

In a literature survey, there have been many researches to allocate radar resource optimally. Reference [3] investigated parameter optimization in the search function with the aim to minimize the required average power for a given search performance. Reference [4] examined the beam overlap impact on probability of detection during a single scan of a phased array radar. Reference [5] showed optimum parameters and performance in constraints applicable for air-to-air surveillance. Reference [6] investigated a particular problem of track maintenance under minimum radar energy conditions. Recently, the problem of target tracking with adaptive update rate has been addressed by many authors [7-9].

Compared with the track-while-search (TWS) tracking that uses scan-to-scan correlation at search illuminations for tracking targets, an ESA radar can use the active tracking which assigns additional track illuminations between search beams and the tracking performance can be improved as a result. Reference [10] showed the performance improvements in active tracking compared to TWS tracking using surveillance performance measure. Reference [11] presented that the active tracking of an ESA radar can provide significantly improved performance over TWS tracking of a MSA radar using Monte Carlo simulation.

In this article, improvement on track formation range in active tracking which assigns additional track illuminations evenly between search illuminations compared to TWS tracking is presented quantitatively. Analytical method using Markov chain with less computational effort is used rather than time-consuming Monte Carlo simulation to be required detailed radar definition. Firstly, Markov chain and track formation range of TWS tracking are shown with the brief explanation of basic theory. Secondly, Markov chain and track formation range of active tracking with one additional track beam are presented with them of the TWS tracking for comparison. It is also given the comparison with respect to the change on the detection probability of the track beam with the proper parameter selection. Moreover, the track formation ranges with various number of additional track beams are compared. In addition, impact on track formation range by the number and detection probability of additional track beams is analyzed simultaneously. Finally, a discussion is given of the proper parameter selection with taking into consideration the number and detection probability of additional track beams.

2. Analysis on Track Formation Range of TWS Tracking

The analysis on detection and tracking range of a radar

† Corresponding Author: College of Informatics, Korea University, Seoul, Korea. (juseoplee@korea.ac.kr)
* Dept. of Computer and Radio Communications Engineering, Korea University/The 3rd R&D Institute, Agency for Defense Development, Korea. (ifrainy@gmail.com)
** The 3rd R&D Institute, Agency for Defense Development, Korea. ({jeroh,sjkim}@add.re.kr)
*** College of Informatics, Korea University, Seoul, Korea. (yskim@korea.ac.kr)
Received: May 2, 2014; Accepted: December 30, 2014

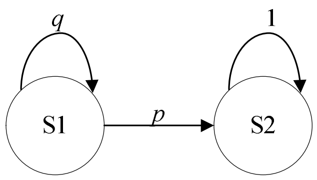

Fig. 1. Markov chain used for the computation of cumulative detection range

system can be carried out conveniently using a Markov chain without using Monte Carlo method at the preliminary system design stage [12]. The Markov chain can be represented generally as follows :

$$\boldsymbol{x}(k+1) = \boldsymbol{F}(k)\cdot\boldsymbol{x}(k) \tag{1}$$

where $\boldsymbol{x}(k)$ is a vector of probabilities (P_i) associated with being in various discrete states(S_i) and $\boldsymbol{F}(k)$ is the transition matrix at time k, respectively. The transition matrix will be a known function of the probability of detection and this probability does not depend upon which states the chain was in before the current state. If the chain is currently in state S_i, then it moves to state S_j at the next step with the corresponding probability in the transition matrix. Thus, given an initial condition vector $\boldsymbol{x}(0)$, succeeding values of $\boldsymbol{x}(k+1)$ can be calculated given $\boldsymbol{x}(k)$. In other words, whether a target is detected after k search scans depends only on detection status after the previous scan and the probability of detection. The Markov chain used for the computation of cumulative detection range in a radar system is shown in Fig. 1 for brief explanation of the basic theory.

S1 and S2 represent the state where no detection has taken place and at least one detection has been made, respectively. The single scan detection probability (p) and q=1-p are functions of time, and thus could be indexed by time instant k, but for notational convenience p and q will not be indexed. The Markov chain can be written as follows:

$$\boldsymbol{x}(k+1) = \boldsymbol{F}(k)\cdot\boldsymbol{x}(k)$$
$$\boldsymbol{F}(k) = \begin{bmatrix} q & 0 \\ p & 1 \end{bmatrix},\ \boldsymbol{x}(0) = \begin{bmatrix} 1 \\ 0 \end{bmatrix} \tag{2}$$

where $\boldsymbol{x}(k)$ is a state vector, containing all state probabilities at time k and $\boldsymbol{F}(k)$ is the transition matrix, describing the transition probabilities between all states at time k.

The cumulative detection range ($R_{d,acc,85}$), where the cumulative detection probability ($P_{d,acc}$) is 85% in the scenario with a decreasing target range from a long distance, can be calculated from (2) as follows:

- The single scan detection probability (p) at time instant k, corresponding to a Swerling I target at the range R_k, is obtained by (3).

$$p = P_{fa}^{\frac{1}{1+SNR}} = P_{fa}^{\frac{1}{1+SNR_{50}\left(\frac{R_{50}}{R_k}\right)^4}} \tag{3}$$

where P_{fa} is the probability of false alarm, R_{50} is the range with the detection probability of 50%, and SNR_{50} is the signal to noise ratio at R_{50} [12].

- $\boldsymbol{x}(k)$ at time instant k is calculated by using (2) and (3) and its second element ($x_2(k)$) is the cumulative detection probability. Then, $R_{d,acc,85}$ is obtained from the corresponding range and the time instant k when $x_2(k)$ is 85%.

Fig. 2 shows the single scan and cumulative detection probability versus range applying above explanation with radar system parameters given in Table 1. The values in Table 1 are used as typical examples for illustration. As shown in Fig. 2, $R_{d,acc,85}$ is about 135km. These single scan and cumulative detection probability are represented as the reference of performance in following comparison figures.

For computation of track formation range of TWS tracking with same parameters in Table 1, the track confirmation criterion is required. In this article, we require 2 detections out of 4 trials followed by 1 detection out of 4 trials. Markov chain used for the computation of track formation range on TWS tracking with this confirmation criterion is shown in Fig. 3 and every trial from S1 to S9 is

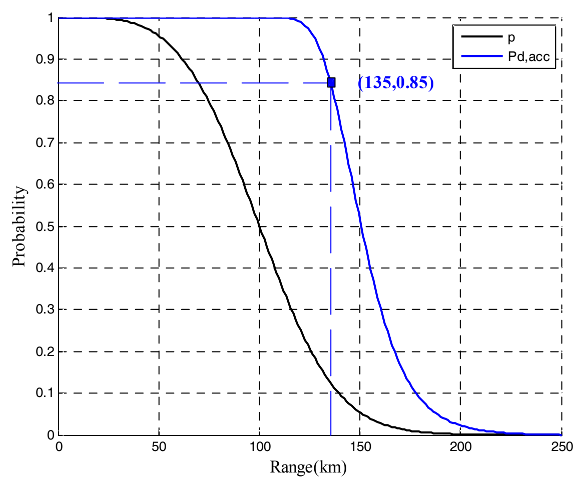

Fig. 2. Single scan and cumulative detection probability versus range

Table 1. Assumed parameters in a radar system

Parameters	Value
R_{50}	100km
P_{fa}	10^{-6}
Ownship velocity	300m/s
Target velocity	-300m/s
Search revisit time	2s
Initial range	250km

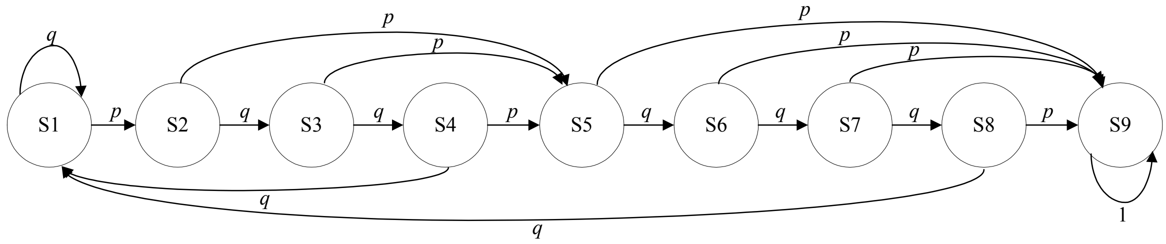

Fig. 3. Markov chain used for the computation of track formation range on TWS tracking with confirmation criterion of 2/4 and 1/4

Table 2. Elements of $\boldsymbol{x}(k)$ and corresponding states in (4)

Elements of $\boldsymbol{x}(k)$	Corresponding States	Elements of $\boldsymbol{x}(k)$	Corresponding States
$X_1(k)$	S1	$x_6(k)$	S6
$x_2(k)$	S2	$x_7(k)$	S7
$x_3(k)$	S3	$x_8(k)$	S8
$x_4(k)$	S4	$x_9(k)$	S9
$x_5(k)$	S5	-	-

performed by search illumination. p and q can be obtained from same method using (3) and the transition matrix and the initial condition vector of this Markov chain can be written as follows:

$$\boldsymbol{x}(k+1) = \boldsymbol{F}(k)\cdot\boldsymbol{x}(k)$$

$$\boldsymbol{F} = \begin{bmatrix} q & 0 & 0 & q & 0 & 0 & 0 & q & 0 \\ p & 0 & 0 & 0 & 0 & 0 & 0 & 0 & 0 \\ 0 & q & 0 & 0 & 0 & 0 & 0 & 0 & 0 \\ 0 & 0 & q & 0 & 0 & 0 & 0 & 0 & 0 \\ 0 & p & p & p & 0 & 0 & 0 & 0 & 0 \\ 0 & 0 & 0 & 0 & q & 0 & 0 & 0 & 0 \\ 0 & 0 & 0 & 0 & 0 & q & 0 & 0 & 0 \\ 0 & 0 & 0 & 0 & 0 & 0 & q & 0 & 0 \\ 0 & 0 & 0 & 0 & p & p & p & p & q \end{bmatrix} \quad (4)$$

$$\boldsymbol{x}(0) = \begin{bmatrix} 1 & 0 & 0 & 0 & 0 & 0 & 0 & 0 & 0 \end{bmatrix}^T$$

Thus, $\boldsymbol{x}(k)$, the 9 by 1 state vector at time instant k, is calculated by using iteratively (3) and (4) for the corresponding range and k. The state variables in (4) are described in Table 2. Because the last element the last element ($x_9(k)$) of the state vector is the track probability (P_t), the track probability of TWS tracking versus range can be depicted as shown in Fig. 4. The track formation range ($R_{t,acc,85}$) of TWS tracking, where the track probability is 85%, is about 105km from Fig. 4.

3. Analysis on Track Formation Range of Active Tracking

For quantitative comparison with track formation range of TWS tracking, Markov chain of active tracking with one track beam between search beams is proposed as shown in Fig. 5. In this article, active tracking that additional track illuminations are evenly distributed between search illuminations is considered. The same track confirmation criterion for TWS tracking (2 detections out of 4 trials followed by 1 detection out of 4 trials) is used and each trial is executed sequentially by search and track illumination, that is, Si states and Ai states. The W1 represents the wait state, an intermediate state in which no action occurs, but that serves to delay the next time an action does occur [12]. T0 is state of having achieved track confirmation. P_s is the detection probability by the search illumination and Q_s is 1-P_s. The calculating method for them is identical to that for p and q. P_a is the detection probability by the track illumination and Q_a is 1-P_a. The transition matrix and the initial condition vector of this Markov chain can be written as (5). The state variables in (5) are described in Table 3.

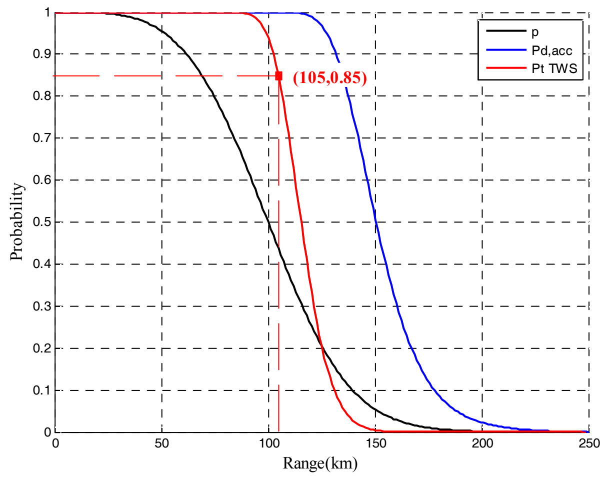

Fig. 4. Track probability of TWS tracking versus range

Fig. 6 shows the comparison of track formation range between TWS and active tracking with one track beam between search beams. The last element ($x_{18}(k)$) of $\boldsymbol{x}(k)$, the 18 by 1 state vector, is used for Fig. 6 because it represents the track probability in this Markov chain relationship. And P_a identical to P_s is also applied in consideration of using same waveform for search and track illumination. Compared with TWS tracking, the improvement in track formation range of about 3.8% is presented because Rt,acc,85 of this active tracking is about 109km.

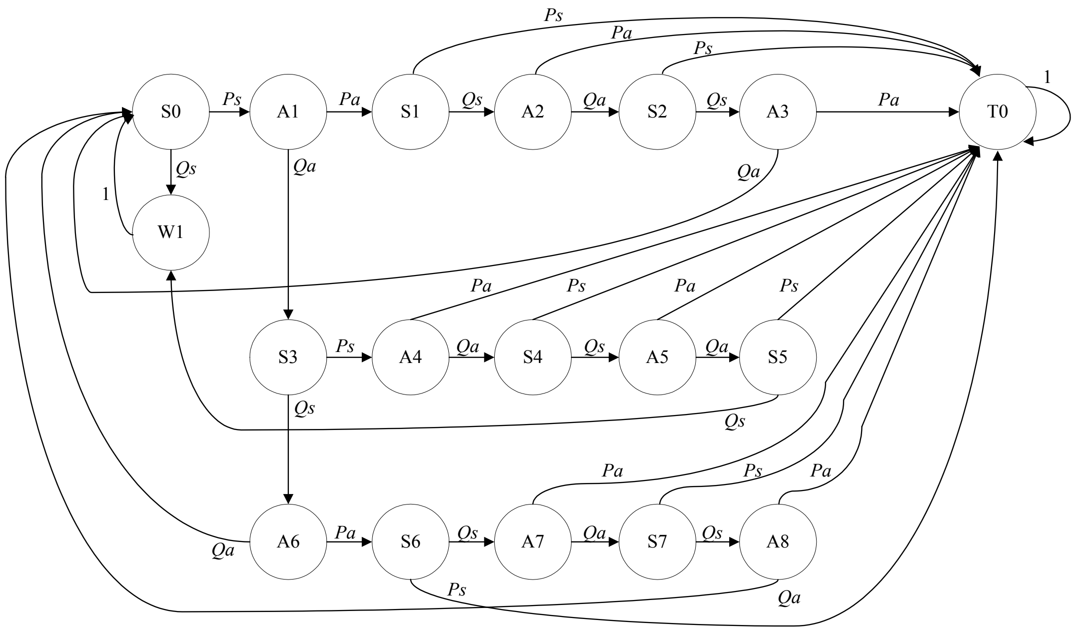

Fig. 5. Markov chain used for the computation of track formation range on active tracking with one track beam between search beams

$$\boldsymbol{x}(k+1)=\boldsymbol{F}(k)\cdot\boldsymbol{x}(k)$$

$$\boldsymbol{F}=\begin{bmatrix}
0 & 1 & 0 & 0 & Q_a & 0 & 0 & 0 & 0 & 0 & 0 & 0 & 0 & 0 & Q_a & 0 & Q_a & 0 \\
Q_s & 0 & 0 & 0 & 0 & 0 & 0 & 0 & 0 & 0 & 0 & 0 & 0 & 0 & 0 & Q_s & 0 & 0 \\
P_s & 0 & 0 & 0 & 0 & 0 & 0 & 0 & 0 & 0 & 0 & 0 & 0 & 0 & 0 & 0 & 0 & 0 \\
0 & 0 & Q_a & 0 & 0 & 0 & 0 & 0 & 0 & 0 & 0 & 0 & 0 & 0 & 0 & 0 & 0 & 0 \\
0 & 0 & 0 & Q_s & 0 & 0 & 0 & 0 & 0 & 0 & 0 & 0 & 0 & 0 & 0 & 0 & 0 & 0 \\
0 & 0 & P_a & 0 & 0 & 0 & 0 & 0 & 0 & 0 & 0 & 0 & 0 & 0 & 0 & 0 & 0 & 0 \\
0 & 0 & 0 & P_s & 0 & 0 & 0 & 0 & 0 & 0 & 0 & 0 & 0 & 0 & 0 & 0 & 0 & 0 \\
0 & 0 & 0 & 0 & P_a & 0 & 0 & 0 & 0 & 0 & 0 & 0 & 0 & 0 & 0 & 0 & 0 & 0 \\
0 & 0 & 0 & 0 & 0 & Q_s & 0 & 0 & 0 & 0 & 0 & 0 & 0 & 0 & 0 & 0 & 0 & 0 \\
0 & 0 & 0 & 0 & 0 & 0 & Q_a & 0 & 0 & 0 & 0 & 0 & 0 & 0 & 0 & 0 & 0 & 0 \\
0 & 0 & 0 & 0 & 0 & 0 & 0 & Q_s & 0 & 0 & 0 & 0 & 0 & 0 & 0 & 0 & 0 & 0 \\
0 & 0 & 0 & 0 & 0 & 0 & 0 & 0 & Q_a & 0 & 0 & 0 & 0 & 0 & 0 & 0 & 0 & 0 \\
0 & 0 & 0 & 0 & 0 & 0 & 0 & 0 & 0 & Q_s & 0 & 0 & 0 & 0 & 0 & 0 & 0 & 0 \\
0 & 0 & 0 & 0 & 0 & 0 & 0 & 0 & 0 & 0 & Q_a & 0 & 0 & 0 & 0 & 0 & 0 & 0 \\
0 & 0 & 0 & 0 & 0 & 0 & 0 & 0 & 0 & 0 & 0 & Q_s & 0 & 0 & 0 & 0 & 0 & 0 \\
0 & 0 & 0 & 0 & 0 & 0 & 0 & 0 & 0 & 0 & 0 & 0 & Q_a & 0 & 0 & 0 & 0 & 0 \\
0 & 0 & 0 & 0 & 0 & 0 & 0 & 0 & 0 & 0 & 0 & 0 & 0 & Q_s & 0 & 0 & 0 & 0 \\
0 & 0 & 0 & 0 & 0 & P_s & P_a & P_s & P_a & P_s & P_a & P_s & P_a & P_s & P_a & P_s & P_a & 1
\end{bmatrix} \quad (5)$$

$$\boldsymbol{x}(0)=\begin{bmatrix}1 & 0 & 0 & 0 & 0 & 0 & 0 & 0 & 0 & 0 & 0 & 0 & 0 & 0 & 0 & 0 & 0 & 0\end{bmatrix}^T$$

Table 3. Elements of $\boldsymbol{x}(k)$ and corresponding states in (5)

Element of $\boldsymbol{x}(k)$	$x_1(k)$	$x_2(k)$	$x_3(k)$	$x_4(k)$	$x_5(k)$	$x_6(k)$	$x_7(k)$	$x_8(k)$	$x_9(k)$
Corresponding State	S0	W1	A1	S3	A6	S1	A4	S6	A2
Element of $\boldsymbol{x}(k)$	$x_{10}(k)$	$x_{11}(k)$	$x_{12}(k)$	$x_{13}(k)$	$x_{14}(k)$	$x_{15}(k)$	$x_{16}(k)$	$x_{17}(k)$	$x_{18}(k)$
Corresponding State	S4	A7	S2	A5	S7	A3	S5	A8	T0

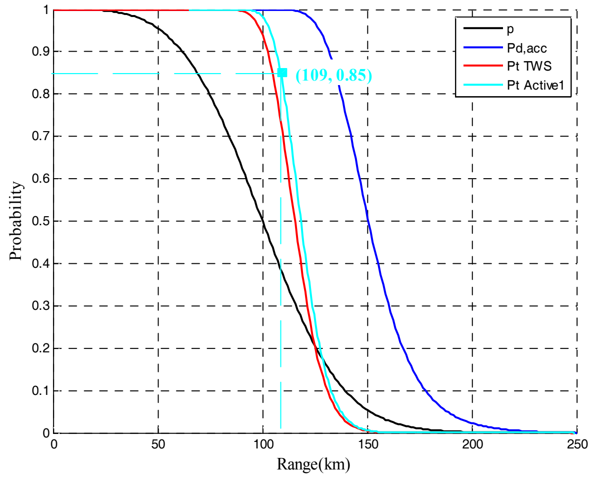

Fig. 6. Comparison of track formation range between TWS and active tracking with one track beam between search beams and P_a identical to P_s

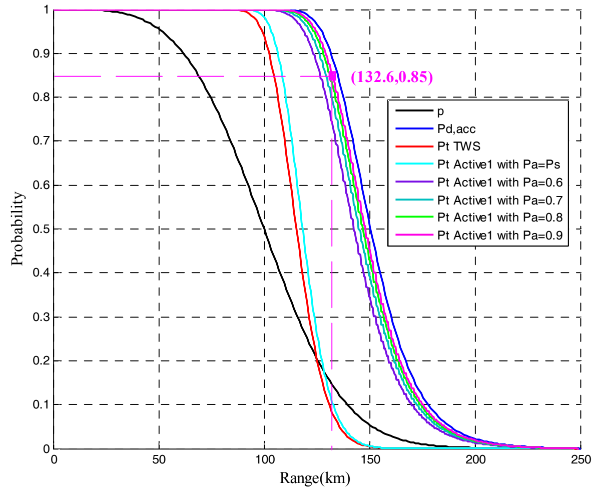

Fig. 7. Comparison of track formation range between TWS and active tracking with one track beam between search beams versus different P_a

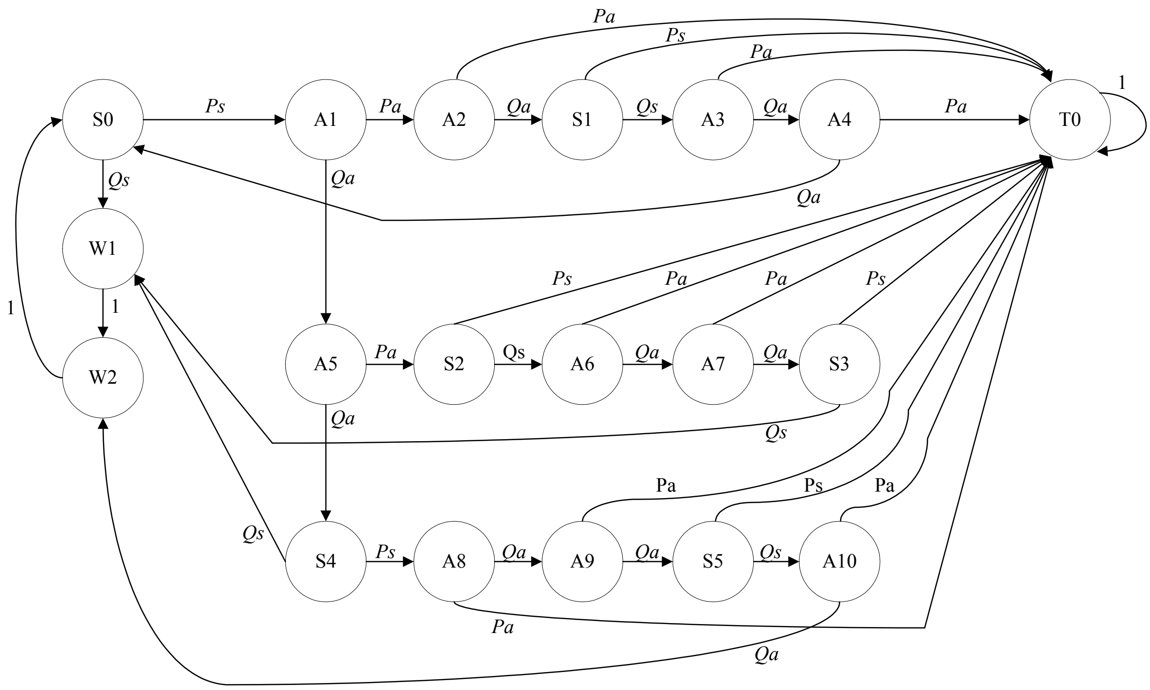

Fig. 8. Markov chain used for the computation of track formation range on active tracking with two track beams between search beams

The higher P_a than the P_s at the same range can be expected by using different waveform for a candidate target [13]. $R_{t,acc,85}$ of active tracking with one track beam between search beams in cases with different P_a from P_s is easily analyzed by using the same Markov chain and the results are shown in Fig. 7. Compared with TWS tracking, the maximum improvement in track formation range of about 26.3% is achieved for P_a of 0.9 because $R_{t,acc,85}$ in this case is about 132.6km.

The track formation ranges of active tracking versus the number of additional track beams between search beams are also analyzed. For analysis, the active tracking with two track beams and three track beams between search beams are considered. The corresponding Markov chains are shown in Figs. 8 and 9, respectively. The same track confirmation criterion for TWS tracking is used for comparison. Si, Ai, and Wi states for search, track, and wait illuminations are shown according to the beam assignment rule for each tracking. The transition matrices and the initial condition vectors of each Markov chain can be written as (6) and (7). The state variables in (6) and (7) are described in Table 4 and 5, respectively.

The last element ($x_{19}(k)$) of $\boldsymbol{x}(k)$, the 19 by 1 state vector in (6), represents the track probability of active tracking

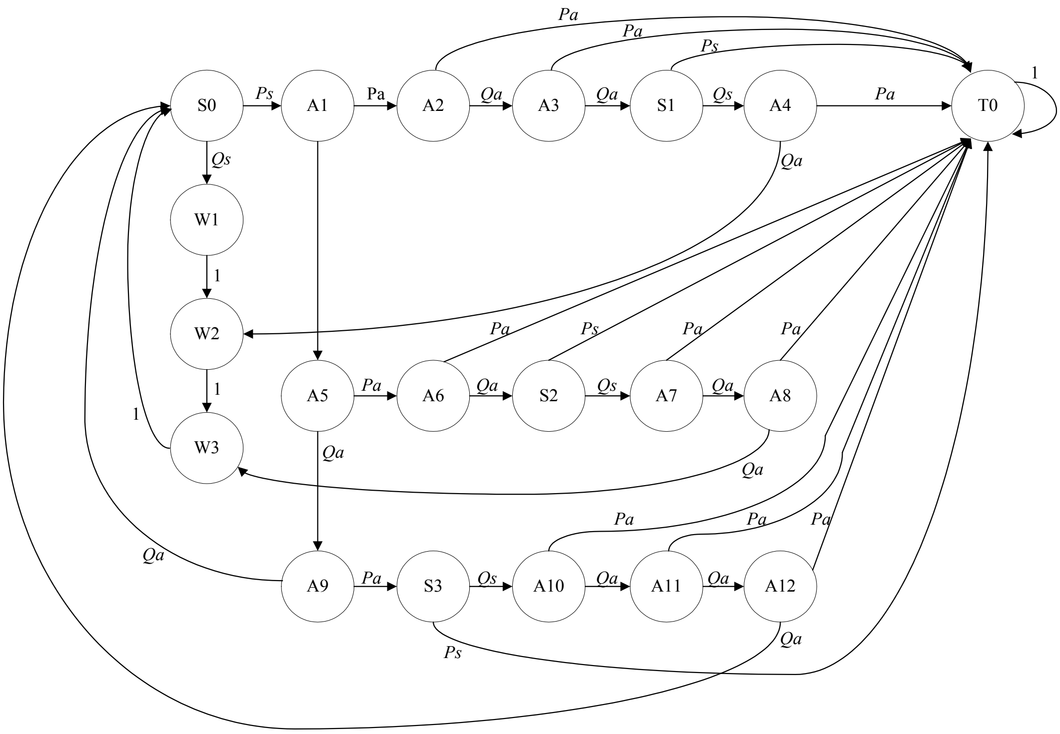

Fig. 9. Markov chain used for the computation of track formation range on active tracking with three track beams between search beams

$$\boldsymbol{x}(k+1) = \boldsymbol{F}(k)\cdot\boldsymbol{x}(k)$$

$$\boldsymbol{F} = \begin{bmatrix}
0&0&1&0&0&0&0&0&0&0&0&0&0&0&0&Q_a&0&0&0\\
Q_s&0&0&0&0&Q_s&0&0&0&0&0&0&0&0&0&0&Q_s&0&0\\
0&1&0&0&0&0&0&0&0&0&0&0&0&0&0&0&0&Q_a&0\\
P_s&0&0&0&0&0&0&0&0&0&0&0&0&0&0&0&0&0&0\\
0&0&0&Q_a&0&0&0&0&0&0&0&0&0&0&0&0&0&0&0\\
0&0&0&0&Q_a&0&0&0&0&0&0&0&0&0&0&0&0&0&0\\
0&0&0&P_a&0&0&0&0&0&0&0&0&0&0&0&0&0&0&0\\
0&0&0&0&P_a&0&0&0&0&0&0&0&0&0&0&0&0&0&0\\
0&0&0&0&0&P_s&0&0&0&0&0&0&0&0&0&0&0&0&0\\
0&0&0&0&0&0&Q_a&0&0&0&0&0&0&0&0&0&0&0&0\\
0&0&0&0&0&0&0&Q_s&0&0&0&0&0&0&0&0&0&0&0\\
0&0&0&0&0&0&0&0&Q_a&0&0&0&0&0&0&0&0&0&0\\
0&0&0&0&0&0&0&0&0&Q_s&0&0&0&0&0&0&0&0&0\\
0&0&0&0&0&0&0&0&0&0&Q_a&0&0&0&0&0&0&0&0\\
0&0&0&0&0&0&0&0&0&0&0&Q_a&0&0&0&0&0&0&0\\
0&0&0&0&0&0&0&0&0&0&0&0&Q_a&0&0&0&0&0&0\\
0&0&0&0&0&0&0&0&0&0&0&0&0&Q_a&0&0&0&0&0\\
0&0&0&0&0&0&0&0&0&0&0&0&0&0&Q_s&0&0&0&0\\
0&0&0&0&0&0&P_a&P_s&P_a&P_s&P_a&P_a&P_a&P_a&P_s&P_a&P_s&P_a&1
\end{bmatrix} \qquad (6)$$

$$\boldsymbol{x}(0) = \begin{bmatrix}1&0&0&0&0&0&0&0&0&0&0&0&0&0&0&0&0&0&0\end{bmatrix}^T$$

Table 4. Elements of $\boldsymbol{x}(k)$ and corresponding states in (6)

Element of $\boldsymbol{x}(k)$	$x_1(k)$	$x_2(k)$	$x_3(k)$	$x_4(k)$	$x_5(k)$	$x_6(k)$	$x_7(k)$	$x_8(k)$	$x_9(k)$	$x_{10}(k)$
Corresponding State	S0	W1	W2	A1	A5	S4	A2	S2	A8	S1
Element of $\boldsymbol{x}(k)$	$x_{11}(k)$	$x_{12}(k)$	$x_{13}(k)$	$x_{14}(k)$	$x_{15}(k)$	$x_{16}(k)$	$x_{17}(k)$	$x_{18}(k)$	$x_{19}(k)$	-
Corresponding State	A6	A9	A3	A7	S5	A4	S3	A10	T0	-

Table 5. Elements of $\boldsymbol{x}(k)$ and corresponding states in (7)

Element of $\boldsymbol{x}(k)$	$x_1(k)$	$x_2(k)$	$x_3(k)$	$x_4(k)$	$x_5(k)$	$x_6(k)$	$x_7(k)$	$x_8(k)$	$x_9(k)$	$x_{10}(k)$
Corresponding State	S0	W1	W2	W3	A1	A5	A9	A2	A6	S3
Element of $\boldsymbol{x}(k)$	$x_{11}(k)$	$x_{12}(k)$	$x_{13}(k)$	$x_{14}(k)$	$x_{15}(k)$	$x_{16}(k)$	$x_{17}(k)$	$x_{18}(k)$	$x_{19}(k)$	$x_{20}(k)$
Corresponding State	A3	S2	A10	S1	A7	A11	A4	A8	A12	T0

$$\boldsymbol{x}(k+1) = \boldsymbol{F}(k)\cdot\boldsymbol{x}(k)$$

$$\boldsymbol{F} = \begin{bmatrix}
0 & 0 & 0 & 1 & 0 & 0 & Q_a & 0 & 0 & 0 & 0 & 0 & 0 & 0 & 0 & 0 & 0 & 0 & Q_a & 0 \\
Q_s & 0 & 0 & 0 & 0 & 0 & 0 & 0 & 0 & 0 & 0 & 0 & 0 & 0 & 0 & 0 & 0 & 0 & 0 & 0 \\
0 & 1 & 0 & 0 & 0 & 0 & 0 & 0 & 0 & 0 & 0 & 0 & 0 & 0 & 0 & 0 & Q_a & 0 & 0 & 0 \\
0 & 0 & 1 & 0 & 0 & 0 & 0 & 0 & 0 & 0 & 0 & 0 & 0 & 0 & 0 & 0 & 0 & Q_a & 0 & 0 \\
P_s & 0 & 0 & 0 & 0 & 0 & 0 & 0 & 0 & 0 & 0 & 0 & 0 & 0 & 0 & 0 & 0 & 0 & 0 & 0 \\
0 & 0 & 0 & 0 & Q_a & 0 & 0 & 0 & 0 & 0 & 0 & 0 & 0 & 0 & 0 & 0 & 0 & 0 & 0 & 0 \\
0 & 0 & 0 & 0 & 0 & Q_a & 0 & 0 & 0 & 0 & 0 & 0 & 0 & 0 & 0 & 0 & 0 & 0 & 0 & 0 \\
0 & 0 & 0 & 0 & P_a & 0 & 0 & 0 & 0 & 0 & 0 & 0 & 0 & 0 & 0 & 0 & 0 & 0 & 0 & 0 \\
0 & 0 & 0 & 0 & 0 & P_a & 0 & 0 & 0 & 0 & 0 & 0 & 0 & 0 & 0 & 0 & 0 & 0 & 0 & 0 \\
0 & 0 & 0 & 0 & 0 & 0 & P_a & 0 & 0 & 0 & 0 & 0 & 0 & 0 & 0 & 0 & 0 & 0 & 0 & 0 \\
0 & 0 & 0 & 0 & 0 & 0 & 0 & Q_a & 0 & 0 & 0 & 0 & 0 & 0 & 0 & 0 & 0 & 0 & 0 & 0 \\
0 & 0 & 0 & 0 & 0 & 0 & 0 & 0 & Q_a & 0 & 0 & 0 & 0 & 0 & 0 & 0 & 0 & 0 & 0 & 0 \\
0 & 0 & 0 & 0 & 0 & 0 & 0 & 0 & 0 & Q_s & 0 & 0 & 0 & 0 & 0 & 0 & 0 & 0 & 0 & 0 \\
0 & 0 & 0 & 0 & 0 & 0 & 0 & 0 & 0 & 0 & Q_a & 0 & 0 & 0 & 0 & 0 & 0 & 0 & 0 & 0 \\
0 & 0 & 0 & 0 & 0 & 0 & 0 & 0 & 0 & 0 & 0 & Q_s & 0 & 0 & 0 & 0 & 0 & 0 & 0 & 0 \\
0 & 0 & 0 & 0 & 0 & 0 & 0 & 0 & 0 & 0 & 0 & 0 & Q_a & 0 & 0 & 0 & 0 & 0 & 0 & 0 \\
0 & 0 & 0 & 0 & 0 & 0 & 0 & 0 & 0 & 0 & 0 & 0 & 0 & Q_s & 0 & 0 & 0 & 0 & 0 & 0 \\
0 & 0 & 0 & 0 & 0 & 0 & 0 & 0 & 0 & 0 & 0 & 0 & 0 & 0 & Q_a & 0 & 0 & 0 & 0 & 0 \\
0 & 0 & 0 & 0 & 0 & 0 & 0 & 0 & 0 & 0 & 0 & 0 & 0 & 0 & 0 & Q_a & 0 & 0 & 0 & 0 \\
0 & 0 & 0 & 0 & 0 & 0 & 0 & P_a & P_a & P_s & P_a & P_s & P_a & P_s & P_a & P_a & P_a & P_a & P_a & 1
\end{bmatrix} \quad (7)$$

$$\boldsymbol{x}(0) = \begin{bmatrix}1 & 0 & 0 & 0 & 0 & 0 & 0 & 0 & 0 & 0 & 0 & 0 & 0 & 0 & 0 & 0 & 0 & 0 & 0 & 0\end{bmatrix}^T$$

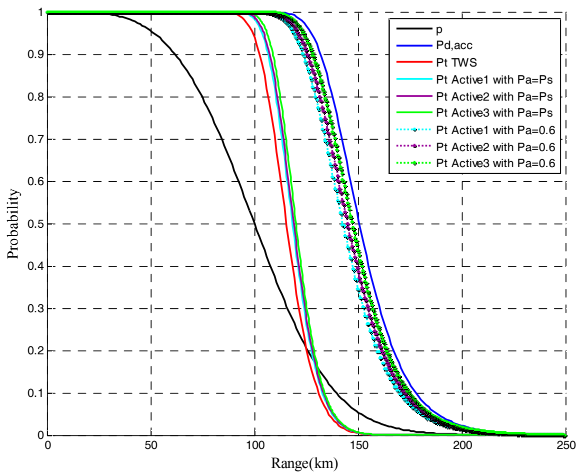

Fig. 10. Comparison of track formation range between TWS and active tracking versus the number of track beams between search beams and P_a

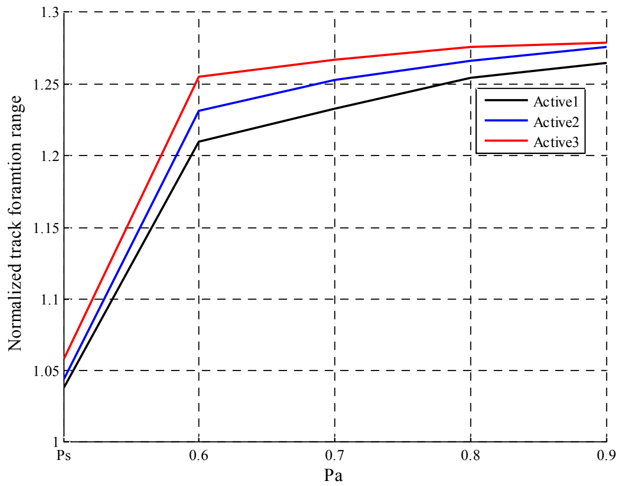

Fig. 11. Normalized track formation range of active tracking based on that of TWS tracking

Table 6. Track formation range of TWS and active tracking with P_a of 0.6 versus the number of track beams between search beams

Tracking method		Track formation range[km]
TWS tracking		105.0
Active tracking	One track beam	126.8
	Two track beam	129.0
	Three track beam	131.5

with two track beams between search beams and the last element ($x_{20}(k)$) of $\boldsymbol{x}(k)$, the 20 by 1 state vector in (7), is that of active tracking with three track beams between search beams. Fig. 10 shows the comparison of track formation range of active tracking versus the number of track beams between search beams in consideration of using same waveform for search and track illumination. The track formation ranges of three active tracking with P_a of 0.6 are also presented in Fig. 10. As depicted in Fig. 10, the number of track beams between search beams has no great impact on the improvement of the track formation range when we use same waveform for search and track illumination. However, the track formation range of active tracking with P_a of 0.6 is improved gradually with respect to the number of track beams between search beams. Compared with TWS tracking, the improvement in track formation range of about 20.8%, 22.9%, and 25.2% is achieved for three active tracking with Pa of 0.6 as given in Table 6.

So far, impact on track formation range by the number and detection probability of additional track beams is analyzed separately. Finally, we take into consideration the number and detection probability of additional track beams simultaneously for discussion on optimized parameter selection. Fig. 11 shows the normalized track formation range of active tracking based on that of TWS tracking. All active tracking cases have the improved track formation range as against that of TWS tracking and maximum improvement of 27.6% is achieved for active tracking with three track beams and P_a of 0.9. It is shown that larger track formation range can be obtained with a given P_a by increasing the number of track beams between search beams. However, it is also shown that track formation range of active tracking with one track beams and P_a of 0.9 is similar to that of active tracking with three track beams and P_a of 0.6. It means the number of track beams becomes less influential as P_a increases.

Generally, more resource is required for a higher detection probability. And the number of track beams is also one of parameters to be needed optimization in radar resource management. Thus, the proper waveform selection for active tracking with a given number of track beams must be carried out from efficient radar resource management perspective. Using the presented analysis method, the consideration of radar resource management can be performed roughly and the range of parameter selection for the optimization can be narrowed to some extent at the preliminary radar system design stage.

4. Conclusion

Compared with the TWS tracking that uses scan-to-scan correlation at search illuminations for tracking targets, a phased array radar can use active tracking which assigns additional track illuminations and the track formation range can be improved as a result. In this article, Markov chains for active tracking which assigns additional track illuminations evenly between search illuminations are presented to show the improved performance quantitatively. Three Markov chains with one, two, and three additional track beams are presented and the performances are obtained without using Monte Carlo simulation. The analysis is carried out with consideration of the detection probability of additional track beams and it is shown that all active tracking cases have the improved track formation range compared with TWS tracking. In addition, it is indicated that analytic selection of the number and detection probability of additional track beams must be carried out for meeting the required track formation range with limited radar resource. Thus, the presented analysis method can be used for reduction to range of parameter selection for the optimization at the preliminary radar system design stage.

References

[1] E. R. Billam, “MESAR-the Application of Modern Technology to Phased Array Radar,” *IEE Tutorial Meeting on Phased Array Radar*, September 1989.

[2] R. Hendrix, “Aerospace System Improvements Enabled by Modern Phased Array Radar-2008,” *IEEE Int. Radar Conf.*, 2008, pp. 275-280.

[3] E. R. Billam, “Parameter Optimization in Phased Array Radar,” *IEEE Int. Conf. on Radar*, 1992, pp. 34-37.

[4] J. E. Fielding, “Beam Overlap Impact on Phased-Array Target Detection,” *IEEE Trans. AES*, vol. 29, no. 2, pp. 404-411, 1993.

[5] P. J. Fielding and A. M. Kinghorn, “Waveform Optimisation for efficient Resource Allocation in Airborne AESA Radar Systems,” *IEE Multifunction Radar and Sonar Sensor Management Techniques,* November 2001.

[6] G. van Keuk and S. S. Blackman, “On Phased-Array Radar Tracking and Parameter Control,” *IEEE Trans. AES*, vol. 29, no. 1, pp. 186-194, 1993.

[7] Y. Boers, H. Driessen, and J. Zwaga, “Adaptive MFR Parameter Control : Fixed against Variable Probabilities of Detection,” *IEE Proceedings-Radar, Sonar, and Navigation,* vol. 153, no. 1, pp. 2-6, 2006.

[8] C. Ting, H. Zi-shu, and T. Ting, “An IMM-Based

Adaptive-Update-Rate Target Tracking Algorithm for Phased-Array Radar," *Int. Symp. on Intelligent Signal Processing and Communication Systems*, November 2007, pp. 854-857.

[9] A. Charlish, K. Woodbride and H. Griffiths, "Information Theoretic Measures for MFR Tracking Control," *IEEE Int. Radar Conf.*, May 2010, pp. 987-992.

[10] T. R. Kronhamn, "AEW Performance Improvements with the ERIEYE Phased Array Radar," *IEEE National Radar Conf.*, 1993, pp. 34-39.

[11] J. R. Hashimi, S. S. Blackman, and S. P. Ickovic, "Simulation of an Air-to-Air Tracking System for an Electronically Steered Antenna," *in Proceedings of the Summer Computer Simulation Conf.*, 1987, pp. 279-284.

[12] S. S. Blackman, *Multiple-Target Tracking with Radar Application*, Artech House, 1986.

[13] S. S. Blackman and R. Popoli, *Design and Analysis of Modern Tracking system*, Artech House, 1999.

Chang-Soo Ahn He received his B.E. and M.E. degrees in electrical engineering from Korea University, Seoul, Korea, in 2002 and 2005, respectively, and is currently working toward Ph.D. degree at Korea University. In 2005, he joined Agency for Defense Development, Daejeon, Korea, where he is currently a senior researcher. His research interests include airborne AESA radar system design and analysis, operational modes design, and radar resource management.

Ji-Eun Roh She received her B.S degree in Computer Science and Engineering from Pusan National University, Korea, and then her M.S. and Ph.D. degrees in Computer Science and Engineering from Pohang University of Science and Technology, Korea, in 2002 and 2006, respectively. In 2006, she joined Agency for Defense Development, Daejeon, Korea, where she is currently a senior researcher. Her research interests include radar signal processing and resource management.

Seon-Joo Kim He received his B.E. and M.E. degrees in electrical engineering from Aju University, Korea, in 1986 and 1988, respectively. In 1988, he joined Agency for Defense Development, Daejeon, Korea, where he is currently a principal researcher. His research interests include airborne AESA radar development and core technologies research.

Young-Sik Kim He received his B.E degree in electronics engineering from Korea University, Seoul, Korea, in 1973, and M.E. and Ph.D. degrees in electrical engineering from the University of Massachusetts at Amherst, in 1986 and 1988, respectively. From 1988 to 1989, he was a Post-Doctoral Research Fellow at the University of Massachusetts at Amherst. From 1988 to 1993, he was with the Mobile Communications Division, Korea Electronics and Telecommunications Research Institute, Daejeon, Korea. In 1993, he joined Korea University, Seoul, Korea, where he is currently a Professor. His research interests include millimeter-wave antennas and front-end systems and mobile telecommunication systems.

Juseop Lee He received his B.E. and M.E. degrees in Radio Science and Engineering from Korea University, Seoul, Korea, in 1997 and 1999, respectively, and Ph.D. degree in Electrical Engineering from The University of Michigan, Ann Arbor, MI, USA, in 2009. In 2001, he joined Electronics and Telecommunications Research Institute (ETRI), Daejeon, Korea, where he was involved in the design of passive microwave equipment for Ku- and Ka-band communications satellites. In 2009, he joined Purdue University, West Lafayette, IN, USA, where he was a Post-Doctoral Research Associate, during which time his activities included the design of adaptable RF systems and invention of field-programmable filter arrays (FPFAs). In 2012, he joined Korea University, Seoul, Korea, where he is currently Associate Professor. His research interests include reconfigurable RF and microwave circuits, satellite transponders, and wireless power transfer.